Cell

Folding and Self-Assembly of the TatA Translocation Pore Based on a Charge Zipper Mechanism

Torsten H. Walther,[1] Christina Gottselig,[1] Stephan L. Grage,[1] Moritz Wolf,[2] Attilio V. Vargiu,[3] Marco J. Klein,[1] Stefanie Vollmer,[1] Sebastian Prock,[1] Mareike Hartmann,[1] Sergiy Afonin,[1] Eva Stockwald,[1] Hartmut Heinzmann,[1] Olga V. Nolandt,[1] Wolfgang Wenzel,[2] Paolo Ruggerone,[3] and Anne S. Ulrich[1,*]

[1]Karlsruhe Institute of Technology (KIT), Institute of Biological Interfaces (IBG-2), Institute of Organic Chemistry and CFN, Fritz-Haber-Weg 6, 76131 Karlsruhe, Germany

[2]KIT, Institute of Nanotechnology and CFN, POB 3640, 76021 Karlsruhe, Germany

[3]Istituto Officina dei Materiali/CNR UOS SLACS and Dipartimento di Fisica, Università di Cagliari, S.P. Monserrato-Sestu Km 0.700, 09042 Monserrato (CA), Italy

*Correspondence: anne.ulrich@kit.edu

http://dx.doi.org/10.1016/j.cell.2012.12.017

SUMMARY

We propose a concept for the folding and self-assembly of the pore-forming TatA complex from the Twin-arginine translocase and of other membrane proteins based on electrostatic "charge zippers." Each subunit of TatA consists of a transmembrane segment, an amphiphilic helix (APH), and a C-terminal densely charged region (DCR). The sequence of charges in the DCR is complementary to the charge pattern on the APH, suggesting that the protein can be "zipped up" by a ladder of seven salt bridges. The length of the resulting hairpin matches the lipid bilayer thickness, hence a transmembrane pore could self-assemble via intra- and intermolecular salt bridges. The steric feasibility was rationalized by molecular dynamics simulations, and experimental evidence was obtained by monitoring the monomer-oligomer equilibrium of specific charge mutants. Similar "charge zippers" are proposed for other membrane-associated proteins, e.g., the biofilm-inducing peptide TisB, the human antimicrobial peptide dermcidin, and the pestiviral E^{RNS} protein.

INTRODUCTION

Electrostatic "charge zippers" are introduced and explored here as a structural principle that can drive the folding and self-assembly of membrane proteins. According to this new concept, extended ladders of salt bridges can form between amphiphilic transmembrane segments and connect them with one another. Several proteins with putative charge zippers motifs have been identified that are involved in diverse cellular processes such as protein translocation, proton transport, antimicrobial action, and molecular recognition. To explain how the idea of a charge zipper emerged and how its existence could be confirmed, we present here our in-depth case study on the Twin-arginine translocase (Tat).

The Tat pathway is dedicated to the transport of fully folded proteins across the membranes of bacteria and plant thylakoids (Fröbel et al., 2012; Mori and Cline, 2001; Palmer and Berks, 2003; Palmer et al., 2005). It requires a much larger pore than the Sec system, through which unfolded proteins are threaded. Tat export is driven by the proton electrochemical gradient (Alder and Theg, 2003). It is essential for many cellular processes (Berks et al., 2005), and in many human pathogens the Tat system is recognized as a virulence factor (Dilks et al., 2003; Zhang et al., 2009). Biotechnologically, it constitutes an important tool for the secretory production of heterologous proteins (Li et al., 2009). In *E. coli* and other Gram-negative bacteria, the minimally active translocation complex consists of three integral membrane proteins TatA, TatB, and TatC. TatC recognizes the cargo protein via a "twin-arginine" containing signal peptide and connects to TatB. TatA occurs in high molar excess and forms the putative translocation pore (Gohlke et al., 2005; Jack et al., 2001; Sargent et al., 2001). It consists of a single transmembrane segment (TMS), followed by an amphiphilic helix (APH), and a densely charged region (DCR) at the C terminus (Lange et al., 2007; Müller et al., 2007; Palmer and Berks, 2003), as illustrated in Figure 1A. Most Gram-positive bacteria and archaea possess only the TatA and TatC components (Dilks et al., 2003; Robinson and Bolhuis, 2004), which are—in contrast to the *E. coli* homologs—substrate specific. For example, *B. subtilis* has two distinct Tat complexes for the two cargo proteins PhoD ($TatA_d/C_d$) and YwbN ($TatA_y/C_y$) (Jongbloed et al., 2004; Pop et al., 2002).

Functionally, TatA has the formidable task to form a large transient pore around the folded cargo protein without allowing protons to leak across the membrane. It has been proposed that TatA self-assembles as an oligomeric ring that opens the pore like a trapdoor (Berks et al., 2000; Chan et al., 2007; Dabney-Smith et al., 2006; Gouffi et al., 2004). This would require a conformational change around a hinge between TMS and APH,

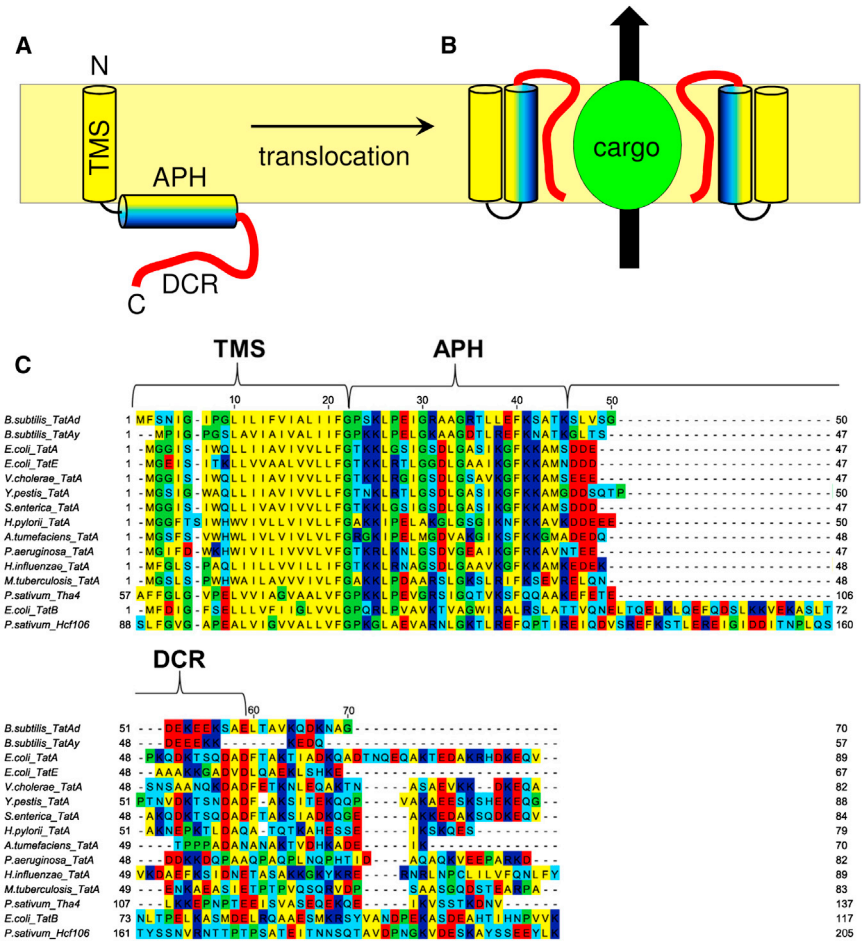

Figure 1. Schematic Illustration and Sequence Alignment of TatA

(A) Schematic illustration of TatA proteins, showing the N-terminal hydrophobic TMS (yellow), the amphiphilic APH (blue) and the unstructured charged C terminus (red).

(B) For translocation, it has been suggested that the TMS of several monomers could assemble as a ring, such that the APH and C termini could fold inward like a trapdoor upon binding the cargo (green).

(C) Sequence alignment of $TatA_d$ from *B. subtilis* with other bacterial and chloroplast proteins, illustrating the conservation of the TMS and APH. Colors are used to illustrate the different types of residues: yellow, hydrophobic (Leu, Ile, Val, Phe, Ala, Met, Trp); red, anionic (Asp, Glu); blue, cationic (Lys, Arg); cyan, polar (Ser, Thr, Gln, Asn, His, Tyr, Cys); green, helix modifiers (Pro, Gly). The last three sequences are truncated. Data were created with the software ClustalW (Larkin et al., 2007) and Jalview (Waterhouse et al., 2009).

as illustrated in Figure 1B. If the amphiphilic helix swings down to align with the TMS, polar residues on the APH would constitute the inner lining of a pore and allow the hydrophilic cargo to pass through. Several other mechanisms of the Tat-dependent translocation have also been proposed, such as a gated pore mechanism (Musser and Theg, 2000), an iris mechanism (Berks et al., 2000), or a membrane weakening and pulling mechanism (Brüser and Sanders, 2003). There exists no experimental evidence yet to support any one of these diverse model.

The variable degree of homo-oligomeric TatA self-assembly represents one of the most intriguing aspects of its function. Gel electrophoresis of the *E. coli* protein in different detergents revealed a ladder of oligomers up to 500 kDa (Oates et al., 2005). In their seminal electron microscopy study of detergent-solubilized TatA, Gohlke et al. have described by single-particle reconstruction a family of cup-shaped complexes (see Figure 4B below), whose inner diameter increases successively from 3 to 7 nm (Gohlke et al., 2005). $TatA_d$ from *B. subtilis* forms 10 nm aggregates when reconstituted in lipid bilayers, and various 150–250 kDa particles were detected in the cytosol upon overexpression in *E. coli* (Barnett et al., 2008; Westermann et al., 2006). In the presence of TatC, the *E. coli* TatA produces tubular structures with 6.7 nm inner diameter in vivo (Berthelmann et al., 2008), whereas TatAB forms homogeneous complexes with an inner diameter of 6 nm (Sargent et al., 2001). The possibility to resolve the atomistic 3D protein structure by X-ray crystallography or nuclear magnetic resonance (NMR) spectroscopy has been challenged by the heterogeneity of the TatA assemblies. All high-resolution information available stems from monomeric $TatA_d$ and fragments thereof. The predicted helical conformation of the TMS and APH was confirmed by circular dichroism (CD) (Porcelli et al., 2002), and the membrane alignment of individual $TatA_d$ segments was determined by oriented CD (Lange et al., 2007). The densely charged C-terminal region was reported to be unstructured, in agreement with previous reports that some truncated TatA/Tha4 analogs remained more or less functional, at least when overexpressed (Dabney-Smith et al., 2003; Lee et al., 2002). Recently, the 3D structure of monomeric $TatA_d$ has been resolved with high resolution by using two complementary NMR strategies. Nuclear Overhauser effect (NOE) constraints and residual dipolar couplings from liquid-state NMR showed that the protein assumes an L-shape structure in detergent micelles, with a putative hinge between the TMS and APH (Hu et al., 2010). Solid-state NMR revealed the orientation of the two helical segments relative to the bilayer normal, confirming that the TMS is aligned essentially upright in the membrane (Müller et al., 2007; Walther et al., 2010). However, the APH of the monomeric $TatA_{2-45}$ construct showed an unexpected oblique tilt angle, in which the charged residues are exposed sideways to the lipid instead of pointing up toward the aqueous layer. It was thus inferred that intramolecular salt bridges could have formed, and that intermolecular salt bridges would also be conceivable (Walther et al., 2010). A recent analysis based on electron spin labeling suggested that the TMS helices are

A

name	sequence of charges along the APH [and TMS]	sequence of charges along the DCR [and C-terminus]	K/R	D/E	net
B.subtilis_TatAd	+.-.+.+.-.+.+.	- - -+- - +.-[.+.- +]	7/2	2/6	+1
B.subtilis_TatAy	+ +.-.+.-.+ -.+.+.	- - -- - + + + - -	8/1	3/6	0
E.coli_TatA	+ +.-.+.+ +.	- - -.+.- +.-[-.+.- +.-.-.+.- -.+ +.- + -]	12/1	10/4	-1
E.coli_TatE	[-.+]+ +.+.-.+.+ +.	- - -.+ +.-.-.- +[.+ -]	10/1	6/3	+2
V.cholerae_TatA	+ +.+.-.+.+ +.	- - -.+ -.-.-[.+.-.+.-.+ + - + -]	11/1	4/7	+1
Y.pestis_TatA	+.+.-.+.+ +.	- -.- +.-.-[.+.- +.+.- -.+.- + -]	10/1	6/5	0
S.enterica_TatA	+ +.-.+.+ +.	- - -.+.- +.-[.-.+.- +.-.+ + - -.+.- + -]	13/0	10/3	0
H.pylorii_TatA	+ +.-.+.+.+ +.+	- - - - -.+.-.+.-[.+.-.-.+.+.-]	12/0	3/8	+1
A.tumefaciens_TatA	+.+.-.-.+.+.+ +.	- -.-.-.+.-.+.-.-[.+]	8/1	6/3	0
P.aeruginosa_TatA	[-.+]+ +.+.-.-.+.+ +.	- - - -- + + -.-[.+.- -.+ + -]	9/3	7/5	0
H.influenzae_TatA	+ +.+.-.+.+ +.+	- - - -+.+.-.-.+.-[.-.+ +.+.+ + - +.+]	13/4	4/5	+8
M.tuberculosis_TatA	+ +.-.+.+.+.-.+	-.-.+.-.-.+.-.-.-[.+]	5/5	3/6	+1
P.sativum_Tha4	… [-.]+ +.-.+.+.+	-.-.-.+ +.-.-[.-.-.+.-.+.+ -]	13/4	1/12	+4
E.coli_TatB	[-.-.]+.+.+.+.-.-.+.-.-.+ +.- +.-.+.- -.+.-.+ +.-.- +.- -.+…		13/5	8/16	-6
P.sativum_Hcf106	… [-.]+.-.+.+.+ -.+ -.-.+ -.+.- + -.- -.+.-.-.+.- -.+.- -.+…		20/8	7/20	+1

B

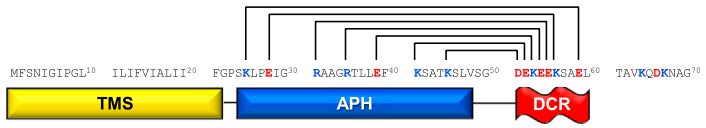

Figure 2. Complementary Charge Motifs in TatA Proteins

(A) The order of charged residues along the predominantly basic APH (blue) is mirrored by the charges along the adjacent, predominantly acidic DCR (red). Residues of the TMS and the ultimate C terminus are included in square brackets, adjacent charges are connected by a "space," and a "dot" stands for any number of interjacent amino acids. (B) Illustration of the seven postulated salt bridges between APH (S24-V48) and DCR (D51-E59) in the sequence of $TatA_d$ from *B. subtilis*, forming an electrostatic charge zipper.

arranged in a line (White et al., 2010), and some weak TMS interactions were detected in a TOXCAT assay (Warren et al., 2009). The same study reports also several genetic mutations, which showed that an acidic motif "DDE" following directly after the APH is important for pore assembly and transport.

Here, we propose a structural model to explain TatA self-assembly and pore formation, based on the available data combined with the new concept that long ladders of salt bridges can connect the molecular segments. Upon inspecting the primary sequence of $TatA_d$, we perceived an intriguing complementarity within the distribution of charged residues along the protein, which turns out to be a conserved property in all homologs. The 70 amino acid $TatA_d$ protein from *B. subtilis* was thus used for model building, MD simulations, and experimental verification of the "charge zipper" concept. To illustrate the possibility that charge zippers may also be present in other membrane-associated proteins, we will round off the discussion with three further case studies: the biofilm-inducing peptide TisB, the human antimicrobial peptide dermcidin, and the pestiviral E^{RNS} protein. The salt bridges predicted from these sequences can be rationalized by the functional roles of the individual proteins. Based on our first results on TatA and the other examples, we thus propose a number of experimentally verifiable hypotheses to be tested by the scientific community.

RESULTS

Complementary Charges along the Primary Sequence

For the sequence alignment of $TatA_d$ from *B. subtilis* with other proteins we used an unbiased set of homologs from interesting Gram-positive and -negative bacteria (Lange et al., 2007) and plant chloroplasts. Figure 1C shows that all proteins are highly charged, despite their transmembrane location. Their extramembraneous domains contain around 40% charged residues (e.g., 17 out of 47 in $TatA_d$), whereas statistically only 22.5% would be expected (5.2% D, 6.3% E, 5.8% K, 5.2% R) (http://prowl.rockefeller.edu/aainfo/struct.htm). Interestingly, the net charge of all TatA proteins is close to zero (except for *H. influenza*). The key observation, on which the entire charge zipper concept is based, is the remarkable finding that the charge patterns along the primary sequence of all TatA homologs exhibit an intrinsic complementarity. Figure 2A displays the order of the charges along the TMS (in square brackets), the APH, and the DCR, plus the remaining C terminus. It is clearly seen that the acidic and basic residues along the APH are inversely mirrored by a complementary motif along the adjacent DCR. This conserved principle typically comprises about seven charge pairs in the various TatA proteins, though the exact pattern of charges differs among the homologs. Details for the case of $TatA_d$ are given in Figure 2B, illustrating the complementary relationships of K25:E59, E28:K56, R31:E55, R35:E54, E39:K53, K41:E52, and K45:D51. As a general observation, the APH carries a net positive charge (and is therefore colored blue in the following figures) and the DCR is acidic (red color). The intrinsic charge complementarity seems to represent a conserved, meaningful structural motif in these evolutionarily optimized membrane proteins. The homology of the bacterial TatA proteins with TatE from *E. coli* and with Tha4 from *A. thaliana* is apparent, but not with TatB or Hcf106.

Self-Assembly of TatA via Charge Zippers

Given the complementary charges on APH and DCR, we propose that these segments can assemble with one another via a "charge zipper" consisting of seven salt bridges. However, in $TatA_d$ the charged region on the APH extends over 21 residues (K25–K45), whereas the DCR contains only nine amino acids (D51–D59). Because the APH is known to be α-helical (Lange et al., 2007; Walther et al., 2010), the characteristic rise of 1.5 Å per residue yields a total length of 31.5 Å. Assuming an extended DCR as a β strand, the characteristic repeat of 3.5 Å per residue would also result in a length of 31.5 Å, which matches perfectly with that of the helix. The remarkable fit of these two complementary elements suggests that an alignment of APH with DCR via salt bridges would be sterically feasible. Given the hydrophobic thickness of a lipid bilayer of around 30 Å, the two structural elements could optimally span the membrane as a hairpin.

The next question concerns the spatial assembly, i.e., whether the flexible DCR can adapt itself smoothly to the rod-like APH

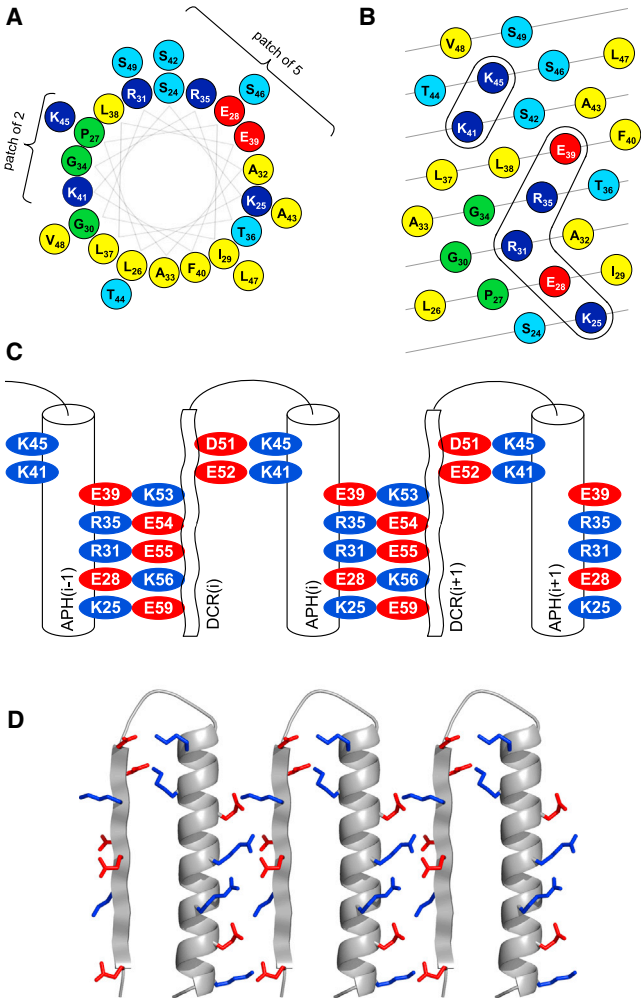

Figure 3. Charge Patches on APH and Postulated Self-Assembly via the DCR

(A) Helical wheel plot of the APH of $TatA_d$, in which the two charge patches are indicated by brackets. The color code is the same as in Figure 1.

(B) Flat projection of the helix surface, with the two charge patches indicated.

(C and D) Schemes of the postulated inter- and intramolecular salt bridges between $APH_{(i)}$ and $DCR_{(i)}$ of molecule $TatA_{(i)}$ with the adjacent $APH_{(i-1)}$, $DCR_{(i+1)}$, etc.

(Figures 3A and 3B). There is obviously no continuous strip of charges along the polar face of the amphiphilic helix. Instead, we recognize two distinct rows of charged residues, namely K41 and K45, as one group, and a second row of K25, E28, R31, R35, and E39. These two charge patches are separated by the bulky hydrophobic L38, which prevents the DCR from lining up with the helix as a continuous band. However, the DCR could readily interact with two APH segments via one of their charge patches each, thus connecting two neighboring TatA monomers. Figures 3C and 3D illustrate schematically how each DCR could form salt bridges with two helices at the same time, and vice versa. (The APHs are viewed here from their polar face, and the TMS segments are not shown). The association of alternating APH and DCR segments as a palisade could explain the self-assembly of $TatA_d$ into oligomers. It cannot be decided at this point whether five intramolecular bridges and two intermolecular ones would be preferred or vice versa. However, our experimental results (see below) indicate that only the arrangement shown in Figures 3C and 3D is plausible, in which two intramolecular salt bridges are formed (K41:E52 and K45:D51) as well as five intermolecular salt bridges between $APH_{(i)}$ and the neighboring $DCR_{(i+1)}$ (via $K25_{(i)}$:$E59_{(i+1)}$, $E28_{(i)}$:$K56_{(i+1)}$, $R31_{(i)}$:$E55_{(i+1)}$, $R35_{(i)}$:$E54_{(i+1)}$, and $E39_{(i)}$:$K53_{(i+1)}$).

The highly charged DCR stretch serves as a flexible strip that connects the amphiphilic APH helices via matching electrostatic interactions. A general geometrical consideration about the DCR as an extended β strand is appropriate at this point. The side chains protrude in an alternating "front-back" pattern relative to the upright β strand in Figure 3D. These side chains on the DCR are principally able to project "left" or "right," as they can rotate freely around their Cβ-Cγ bond. Therefore, no particular torsional strain is expected along the β stranded backbone of the DCR when the TatA molecules are being zipped up. The APH···DCR-APH···DCR-APH palisade in Figure 3D is drawn flat in the plane of the paper, but it could just as readily form a concave wall. The flexible side chains engaged in the salt bridges should make it easy to adjust the curvature. Most importantly, the resulting palisade has an overall amphiphilic structure, with a polar face carrying the salt bridges (facing the viewer of Figures 3C and 3D), and a hydrophobic backside consisting of the apolar residues on the APH segments. This flexible amphiphilic character suggests that the palisade could be accommodated in two ways in the membrane: (1) flat on the bilayer surface (e.g., in the resting state of the translocase), and (2) it could also become immersed as a curved transmembrane pore during translocation.

Next, we may speculate about the possible mechanism of pore formation, starting with monomeric TatA units that are anchored in the lipid bilayer by their TMS. Figure 4A illustrates how they could be preassembled side-by-side (Warren et al., 2009; White et al., 2010), such that the amphiphilic palisade comes to lie flat on the bilayer surface. The palisade would form an extended polar platform on the membrane, ready to receive the cargo protein from TatC. The TatA row could spiral around the cargo, or it could line up with another row by making contact either via the tips of the hairpins (front-to-front) or via the TMS (back-to-back). In either arrangement, the palisade(s) carrying the cargo could then flip into an upright transmembrane alignment, surrounding the cargo and shielding it from the lipids, allowing it to escape from the cell. The diameter of the hydrophilic circle or slit that is transiently formed across the membrane would thus be determined by the size of the folded cargo protein.

This speculative translocation process would be compatible with the trapdoor mechanism discussed in the literature (Berks et al., 2000; Chan et al., 2007; Dabney-Smith et al., 2006; Gouffi et al., 2004) (see Figure 1B). If the palisade wraps itself around the cargo, or if two TatA rows assemble front-to-front, the hairpins would have to swing into the membrane by a flexible hinge between TMS and APH. Alternatively, in the case of a back-to-back assembly, the TatA proteins could retain a rigid L-shape and cooperatively slide backward into the lipid bilayer. Given the available EM data of an oligomeric TatA complex

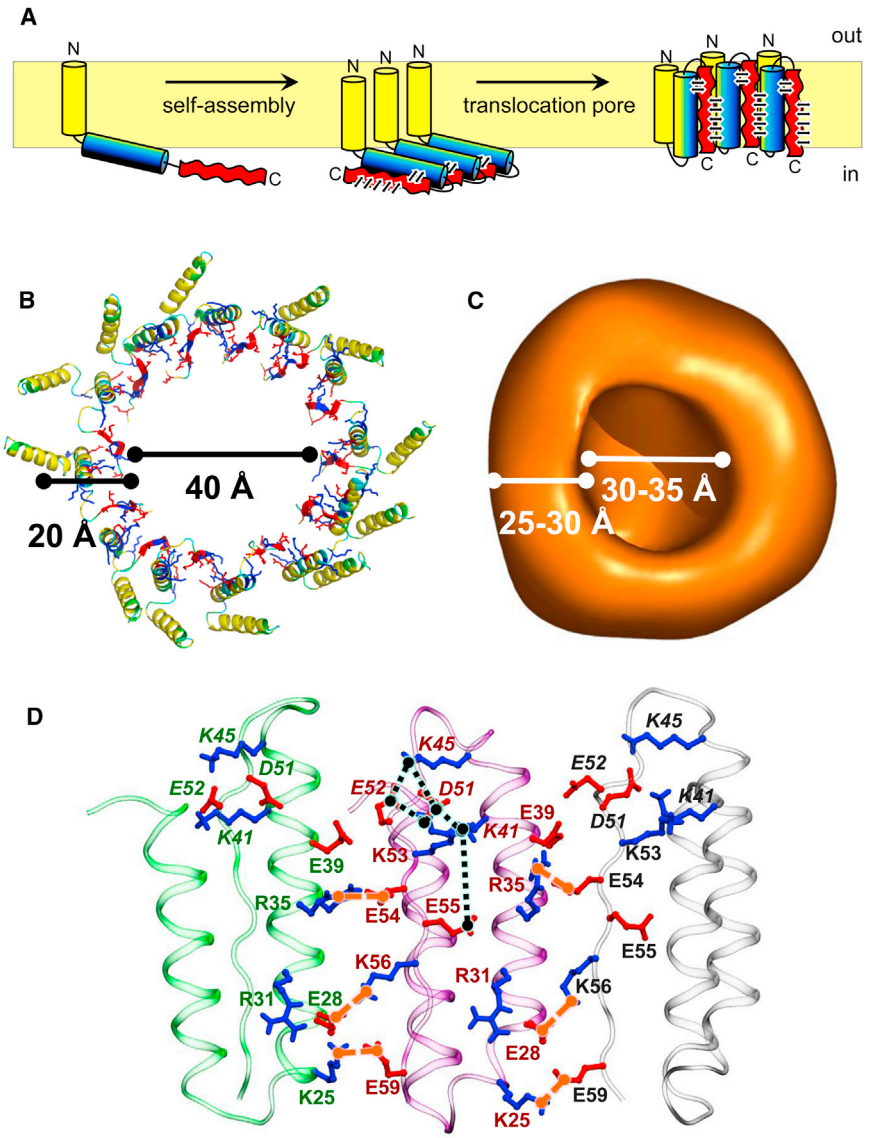

Figure 4. Molecular Dynamics Simulations of Oligomeric TatAd

(A) Illustration how TatA might preassemble to form an amphiphilic palisade, which can get immersed into the membrane during translocation.

(B) Structure-based Gō model of a dodecameric pore in a hydrophobic slab, which was assembled via charge zippers as constraints (see Figure S1 for starting conditions). Same color code as in Figure 1.

(C) Low-resolution 3D model of a detergent-solubilized TatA pore complex obtained with electron microscopy by Gohlke et al. (2005). Copyright 2005 National Academy of Sciences, USA.

(D) Representative snapshot from a further series of unbiased all-atom MD simulations in implicit solvent, started with three monomers (green, purple, and gray) that were extracted from the Gō model above (see Figure S2 for starting conditions). Charged residues are shown in sticks, and the inter- and intramolecular salt bridges with an occupancy larger than 10% are highlighted by orange and black dashed lines respectively. See also Figures S1 and S2, Tables S1 and S2, and Movie S1.

(Gohlke et al., 2005), we have chosen the trapdoor mechanism to model an open TatA pore below. Yet, this does not imply any ab initio preference for either mode of translocation. The main point is that the cargo protein would always face the polar side of the amphiphilic palisade, which can span the membrane during the moment of translocation.

MD Simulations of Self-Assembled TatA

To assess whether our postulated charge zipper model is compatible with a stable tertiary and quaternary structure of a self-assembled $TatA_d$ pore, we performed MD simulations using a structure-based Gō model (Gō and Scheraga, 1976) [see Extended Experimental Procedures for details]. The known helical conformation of the TMS and APH were implemented as constraints (see Figure S1A), together with the postulated intra- and intermolecular contacts of the salt bridges. To model a circular pore, the Gō simulations were started with 12 isolated $TatA_d$ molecules far apart in a hydrophobic-slab as an implicit membrane (see Figure S1B). Using an annealing protocol, we observed in repeated MD runs the formation of a stable $TatA_d$ dodecamer featuring the postulated salt bridges (see Movie S1). The resulting complex forms a proper pore with a hydrophilic lining and a hydrophobic outer surface that is membrane-embedded (Figure 4B). The inner diameter of about 40 Å and the outer diameter of 80 Å fit very well to the dimensions of the circular TatA complex from *E. coli,* consisting of 12–14 subunits as described by electron microscopy at low resolution (Figure 4C)(Gohlke et al., 2005). The size of known Tat substrates ranges between 20 Å and 70 Å (Berks et al., 2000), hence a medium-size cargo protein would fit through the putative dodecameric model. In principle, any variable number of TatA monomers can be zipped up to form a pore, which would explain for the first time the versatility in pore sizes described in the literature (Gohlke et al., 2005; Leake et al., 2008).

The structure-based Gō model does not provide an unbiased view on the stability of the salt bridges in the TatA complex because they were implemented as constraints. We therefore performed another series of unbiased all-atom MD simulations on three adjacent TatA monomers, extracted from the dodecameric Gō model as a starting structure (see Figure S2 for starting conditions, and Extended Experimental Procedures for details on the simulation protocol). A representative snapshot of these MD results in implicit solvent is illustrated in Figure 4D,

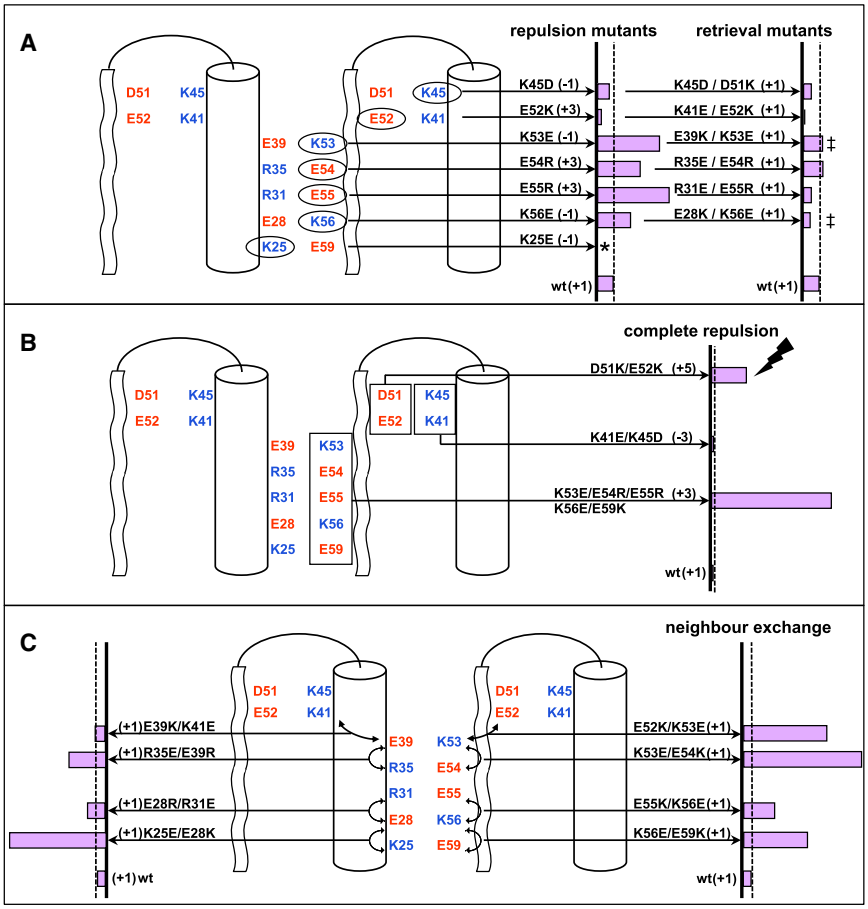

Figure 5. Effect of Specific Charge Mutations

The monomer/oligomer ratio of $TatA_d$, as examined by blue native gel electrophoresis and determined quantitatively from the band intensities of the corresponding western blot.

(A) Single charge repulsion mutants and retrieval mutants. The asterisk marks one mutant that did not express. Mutants marked with ‡ are scaled according to repetition experiment (see Figure S3C).

(B) Complete repulsion mutants. The flash marks one mutant that disassembled unexpectedly, but which can be attributed to the high charge of +5 in this monomer (in brackets).

(C) Neighbor exchange mutants, in which the total protein charge is kept unchanged.

See also Figures S3 and S4 and Table S3.

demonstrating that the proposed self-assembly of TatA and the covalent loop arrangements are indeed sterically feasible. Furthermore, a statistical analysis of the trajectories suggests that the electrostatic contacts are interchanging rapidly throughout the simulation. The statistical occurrences of the observed pairwise interactions are listed in Table S2. Out of the five salt bridges proposed to be involved in intermolecular interactions, K25:E59, E28:K56, and R35:E54 were indeed remarkably stable during the MD run. E39:K53 occurred only temporarily because the respective intramolecular interaction was found to be much more prevalent. R31 did not engage in the proposed intermolecular interaction with E55, but instead it associated temporarily with E54 during the simulation. E55 was in turn engaged in an intramolecular salt bridge with K53, which also participated in a cluster (E52, D51, K45, and K41) that stabilizes the hairpin between APH and DCR. This intramolecular cluster contains multiple forked salt bridges, rather than the two discrete postulated pairs K41:E52 and K45:D51. Such "complex" salt bridges in proteins are well known in the literature (Musafia et al., 1995). MD simulations have thus demonstrated that the salt bridge patterns in the charge zippers are not static and strictly pairwise as originally postulated, but instead they are highly dynamical. By being able to interchange continually, these "fuzzy" charge zippers maintain an overall charge balance over the polar face of the oligomeric TatA assembly, allowing them adapt to the local surface of any cargo molecule in passing.

Experimental Evidence for the Structural Relevance of Charge Zippers

To validate the charge zipper experimentally, we prepared a series of specific charge mutations and monitored their effect on $TatA_d$ self-assembly. For each mutant, the monomer-oligomer equilibrium was examined in blue-native gel electrophoresis (BN-PAGE), as introduced by Warren as a qualitative assay (Warren et al., 2009). TatA from *E. coli* is known to migrate as a characteristic ladder ranging from well below 100 kDa to over 500 kDa (Oates et al., 2005). Because BN-PAGE uses mild detergents to extract the proteins from the cellular membranes, this ladder supposedly represents the naturally occurring oligomers of preassembled TatA complexes. According to the charge zipper hypothesis, we expect that the inversion of a single charge within an intermolecular salt bridge will destabilize the complex and shift the ladder toward the monomeric or low-molecular weight fractions. A second, compensatory charge inversion should then be able to restore the original pattern on the gel. Mutations in the postulated intramolecular salt bridges, on the other hand, should not influence the monomer-oligomer equilibrium to such extent. We systematically examined all postulated pairs of charges, targeting either the APH or the DCR region. The original gels are collected in Figures S3 and S4. The results are summarized in Figure 5, where we refined the assay by analyzing the intensities of the monomeric versus oligomeric bands in order to quantitatively measure the degree of $TatA_d$ disassembly. The resulting monomer/oligomer ratios of the charge mutants are displayed as bars in relation to the wild-type reference that was run on the same gel (dashed line). The long bars for K53E, E54R, E55R, and K56E in Figure 5A clearly show that all repulsion mutations in the patch of five salt bridges lead to increased disassembly

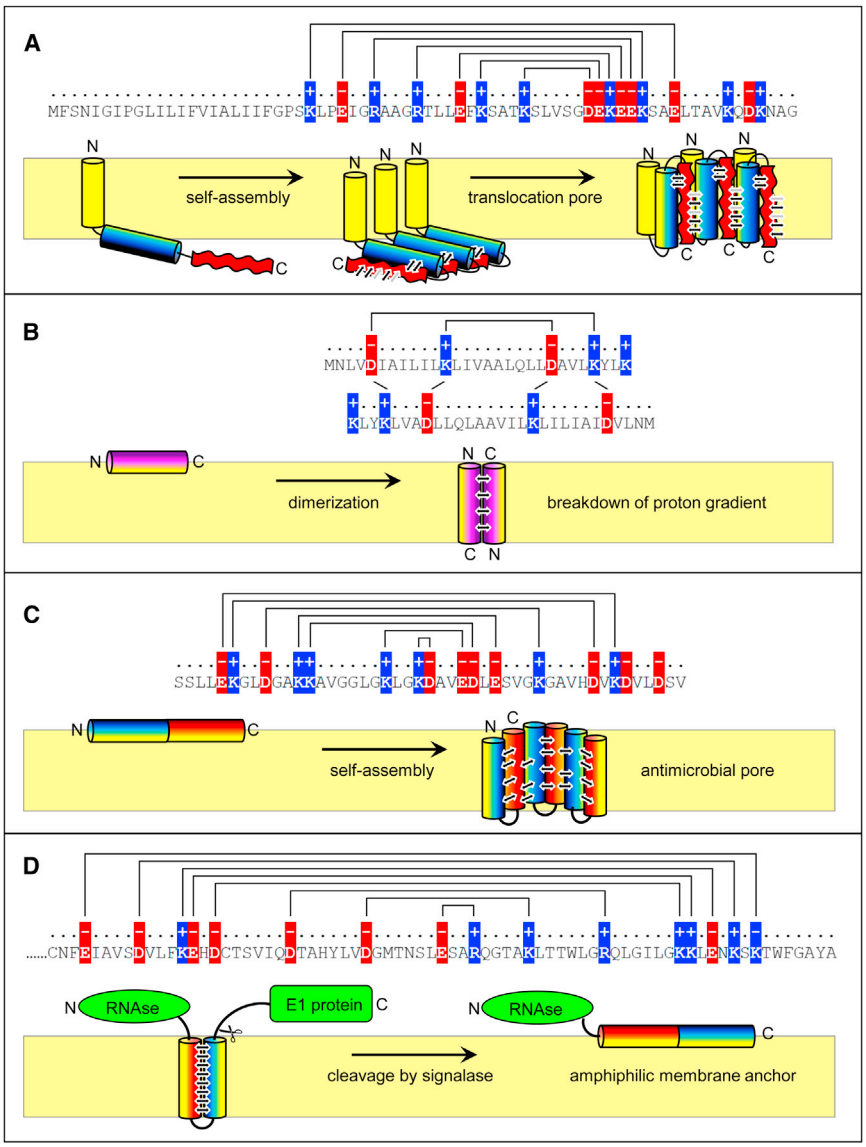

Figure 6. Postulated Charge Zippers in Membrane-Associated Proteins

Postulated charge zippers in (A) TatA, (B) TisB, (C) Dermcidin, and (D) E^{RNS}.

of TatA, as predicted. The single charge repulsion mutations within the patch of two salt bridges (K45D and E52K), on the other hand, did not show any effect on the oligomerization behavior, as expected. We may thus conclude that the patch of five salt bridges is predominantly engaged in intermolecular interactions, and the patch of two in an intramolecular cluster (as used above for the model building in Figure 3C). Next, we inverted also the partner charge within each of the postulated salt bridges. The short bars for all retrieval mutants in Figure 5A show that the stability of the original oligomeric state of TatA was successfully recovered for the intermolecular contacts and maintained for the intramolecular ones, as expected from the charge zipper model.

To see the largest possible effect, we then disrupted all of the postulated salt bridges within the patch of five at the same time, and within the patch of two. As expected, Figure 5B shows that the intermolecular 5-fold charge repulsion mutant (K53E-E54R-E55R-K56E-E59K) disassembled essentially into monomers, whereas the 2-fold mutant K41E-K45D showed no destabilization of the oligomer, being part of the intramolecular cluster. The only unexpected result is seen for the 2-fold charge repulsion mutant D51K-E52K, which disassembles significantly (marked by a flash in Figure 5B). This inconsistency is very likely explained by the total charge of the resulting $TatA_d$ molecules, which is listed in brackets for each of the mutants in Figure 5. Starting with a net charge of +1 for the wild-type protein, most of the mutations resulted in a total charge of −1 or +3, which seems to be tolerated in the oligomeric state. Only the inconsistent 2-fold charge repulsion mutant D51K-E52K gained a net charge of +5, which leads to considerable electrostatic repulsion between the monomers and thereby prevents self-assembly. To avoid any such influence of net charge in the disassembly assay, we performed another series of mutations that kept the total charge on $TatA_d$ unchanged. To this end, any two neighboring charges along the primary protein sequence were interchanged, moving up the APH and down again along the DCR, as seen in Figure 5C. According to the simple charge zipper hypothesis, all these mutations should perturb the intermolecular zipper and thereby lead to increased disassembly. Indeed, the long bars - compared to the wild-type - demonstrate that seven out of eight neighbor exchange mutants behave as expected, with increased monomer/oligomer ratios.

The most important conclusions from both, the mutation experiments and the MD analysis, can thus be summarized as: (1) the charge zipper motif has a structurally relevant role in TatA folding and self-assembly, (2) it can explain the formation of a translocation pore with variable size, and (3) it is a "fuzzy" zipper rather than a discrete ladder of complementary charge pairs, in which (4) salt bridges K25:E59, E28:K56, and R35:E54 are mainly responsible for the intermolecular connections, and (5) residues K41, K45, D51, and E52 are involved in an intramolecular cluster that can dynamically include also K53 and E55. A schematic model of TatA self-assembly and pore formation is illustrated in Figure 6A, in which the important salt bridges are shown as black double-headed arrows and the less prominent

ones as gray. For clarity, only three TatA monomers are illustrated.

Potential Charge Zipper Motifs in Other Proteins

The terms "charge zipper," "salt bridge zipper," "electrostatic zipper," and "ionic zipper" have occasionally been used in the past to describe globular protein structures but in a less stringent context. For example, it was noted that the interface between subunits of the pyruvate dehydrogenase multienzyme complex consists of salt bridges (Frank et al., 2005; Mande et al., 1996), that the MD-driven unfolding of the adenylate kinase involves the successive rupture of salt bridges (Beckstein et al., 2009), or that myosin VI dimerizes via several salt bridges (Kim et al., 2010). Also the interaction between overall positively and negatively charged regions has been denoted as "zippers," e.g., the binding of filaggrin to intermediate filaments (Mack et al., 1993), or the dimerization of the microtubule-associated tau protein (Rosenberg et al., 2008). However, none of these cases showed any correlation between primary sequence and 3D protein structure, and ab initio prediction or model building was out of reach for these globular proteins. In the present work, on the other hand, primary sequence analysis and simple architectural principles lie at the very core of our advanced definition of charge zippers. The linear ladder of intra- and intermolecular salt bridges between the APH and the DCR of $TatA_d$ therefore represents a novel structural motif in proteins.

A characteristic aspect of the charge zipper in TatA is the linear relationship between the charges along the primary protein sequence, which can be mapped directly onto the two complementary secondary structure elements. Based on this simple principle, we scanned the Uniprot database with about 533,000 annotated sequences. Almost 400,000 proteins carry a putative charge zipper motif with a length of five or more pairs of complementary charges in a row. The vast majority of these are obviously due to a statistically coincidental pattern of charged amino acids, and further constraints are needed to narrow them down to a meaningful family. To nevertheless illustrate the general potential of the charge zipper hypothesis, we present here a few hand-picked examples, of which we suppose that the postulated charge zippers are structurally and functionally meaningful. The following representatives are illustrated in Figure 6, and will be rigorously tested in the future.

TisB is a small "toxic protein" from *E. coli*, involved in stress response via the TisB-IstR toxin/antitoxin system. Interaction of the highly charged, amphiphilic helix with the inner bacterial membrane has been shown to uncouple the pH gradient and deplete ATP levels (Dörr et al., 2010; Unoson and Wagner, 2008). The resulting metabolic shutdown drives the bacteria into dormancy and leads to the formation of persister cells, which can revive in the form of biofilms. Our first experiments using oriented circular dichroism and coarse-grained MD simulations suggest that the amphiphilic TisB helix favorably inserts in a transmembrane alignment (Steinbrecher et al., 2012). Remarkably, it does not form pores, but it slowly equilibrates a proton gradient in vesicle permeation assays. We thus propose that membrane-inserted TisB assembles as an antiparallel dimer via a charge zipper consisting of four salt bridges, as illustrated in Figure 6B. The polar interface of the dimer could pull water molecules into the hydrophobic bilayer core, which would decrease the activation barrier for protons or hydroxide ions to pass across the membrane or to neutralize each another. This way, the charge zipper model could explain the molecular trigger for biofilm formation.

Dermcidin is a protein secreted in human sweat that gets cleaved into several fragments, which exhibit antimicrobial activity against bacterial membranes (Schittek et al., 2001). The most prominent one, DCD-1L, is shown in Figure 6C. By using oriented CD and patch clamp, we have found that it binds to the membrane surface as an amphiphilic helix and that it can form pores (Paulmann et al., 2012). However, the DCD-1L helix is much too long—by a factor of two—to span the lipid bilayer in a transmembrane alignment. We therefore postulate that the predominantly cationic N-terminal half (blue gradient, 23 amino acids) can fold back on the predominantly anionic C terminus (red gradient, 24 amino acids) to form a helical hairpin. The resulting pore would then be stabilized by charge zippers consisting of seven intra- and intermolecular salt bridges per monomer.

The E^{RNS} protein from the bovine diarrhea pestivirus is anchored to the membrane surfaces (endoplasmic reticulum and plasma membrane) of the infected host cell by a long amphiphilic C-terminal helix, as shown on the right-hand side of Figure 6D (Tews and Meyers, 2007). This region serves as an intracellular retention signal for the virulence factor that acts via its catalytic RNase domain (Burrack et al., 2012). E^{RNS} is produced as part of a long polyprotein precursor (E^{RNS}-E1-E2) that must get cleaved by a protease (scissor symbol), but the signalase is known to recognize only transmembrane segments. Therefore, we postulate that the C-terminal segment of E^{RNS} should be able to fold transiently into a helical hairpin that is stabilized by a charge zipper consisting of up to eight salt bridges.

DISCUSSION

The proposed mechanistic model of $TatA_d$ from *B. subtilis* is based on a straightforward attempt to fold the primary sequence of this integral membrane protein into a functionally plausible 3D structure. Having noticed that a conserved pattern of charges in the protein sequence may lead to the formation of an electrostatic "charge zipper," all subsequent arguments are based on simple criteria of sequence homology, charges, hydrophobicity, hydrogen-bonding, and steric volume. Essentially, the amphiphilic α-helix of TatA can fold into a hairpin with the adjacent β stranded region, stabilized by a cluster of intramolecular salt bridges. One hairpin can be connected to another via a ladder of intermolecular salt bridges, yielding an amphiphilic palisade. As the palisade has an appropriate height to span the membrane, we suggest that it constitutes the hydrophilic lining of the (transient) translocation pore.

Independent support for this fundamental role of electrostatic interactions in TatA comes from a recent study by van der Ploeg, who report a peculiar salt dependence for protein translocation (van der Ploeg et al., 2011). Numerous mutants of $TatA_y$ from *B. subtilis* lost their function when grown in a medium containing 1% NaCl, but they facilitated secretion in a low-salt medium. The same effect was also observed for *B. cereus* and *S. aureus*. The

intriguing destabilization of the translocase by NaCl can now be rationalized in terms of the charge zipper concept because electrostatic interactions are obviously weakened by high salt concentrations.

To support the steric feasibility of our proposed $TatA_d$ structure, we used structure-based Gō simulations to construct a circular dodecameric pore complex in the membrane. Further all-atom MD simulations provided direct support for the local contacts between the postulated salt bridges, providing important insights into their highly dynamic nature. Experimental evidence for the postulated intra- and intermolecular salt bridges in $TatA_d$ was finally obtained by monitoring the effect of specific charge mutations on the monomer-oligomer equilibrium in blue-native gel electrophoresis. The inversion of a single charge in one of the *inter*molecular salt bridges caused the oligomeric protein to disassemble into monomers, whereas a charge inversion in an *intra*molecular bridge did not, as expected. By inverting also the apposed charge in these mutants, the original oligomeric state of TatA could be recovered. Together with further multiple repulsion and neighbor exchange mutations, these experiments have validated the key role of electrostatic charge zippers in TatA folding and self-assembly. Analogous working models are presented for several other membrane proteins. In the following, we propose some structural and mechanistic hypotheses, addressing also some of the remaining open questions, which can now be rigorously tested.

Hypothesis 1 on TatA Homologs

In $TatA_d$ from *B. subtilis* the pattern of charged residues along the APH is perfectly complementary to the DCR, but in other homologs there are several deviations (see Figure 2A). If we allow for "fuzzy" charges zippers, however, as suggested by the MD analysis, these imperfections can still be reconciled with a stable complex due to the high number of matching contacts. Analogous charge zippers should thus be found also in the other TatA homologs.

Hypothesis 2 on Site-Directed Mutations

Transport assays have shown that the acidic DDE motif of TatA from *E. coli* is functionally relevant (Warren et al., 2009). No effect was seen when a single amino acid was substituted, but translocation and self-assembly were substantially reduced when all three residues were changed simultaneously. According to the charge zipper model, this DDE motif (of *E. coli*) should be involved in an intramolecular electrostatic cluster, which is less sensitive to disassembly. The triple mutations NNQ or LLM in *E. coli*, on the other hand, would not only cause a major disruption of the salt bridges but also change the net charge of the protein (as seen for D51K/E52K in Figure 5B). It would thus be interesting to see whether an inversion of the partner charges of the DDE motif could retrieve function. We note, however, that functional translocation assays might suffer from complications if the mutations affect any interactions of TatA with TatC or the signal peptide.

Hypothesis 3 on Structure Analysis

We have argued that different numbers of TatA monomers can assemble in a circular pore. TatA from *E. coli* is known to assemble dynamically into complexes with variable stoichiometry in response to the cargo protein (Leake et al., 2008), and its low-resolution electron microscopy of detergent-solubilized TatA revealed cavernous complexes of different sizes (Gohlke et al., 2005). It would now be interesting to fit the charge zipped TatA complexes into the 3D density maps with a suitable number of monomers (see Figure 4). It is conceivable that the lid-like structures described in these reconstructions can be attributed to the last 33 amino acids of TatA from *E. coli*, which has a longer C terminus than the *B. subtilis* protein with only an additional 10 amino acids after the DCR (which were left out in our model). Furthermore, crystallization trials could be set up with rationally truncated proteins, in which either the last few C-terminal residues are removed up to the DCR motif, or the use of suitable amphipols may allow removal of the N-terminal TMS.

Hypothesis 4 on Translocation

One of the most intriguing questions emerging from our model is concerned with the geometry of the preassembled TatA palisade and its transient membrane immersion during the process of translocation. A self-assembled row of TatA (as postulated in Figure 6A) could interact with the cargo protein either by encircling it to form a pore or as a slit if two TatA rows are assembled front-to-front or back-to-back. The active trapdoor mechanism would require a conformational change around a flexible hinge between TMS and APH, whereas a passive sliding slit mechanism would be compatible with a rigid TatA structure. The molecular flexibility of TatA and the morphology of membrane-bound oligomers thus need to be examined in more detail.

EXPERIMENTAL PROCEDURES

Structure-Based Gō Models

Simulations of oligomeric TatA were performed using structure-based models (Whitford et al., 2009) with GROMACS 4.0 (Hess et al., 2008) and the PLUMED plugin (Bonomi et al., 2009). The parameters generated using SMOG (Noel et al., 2010) from the starting conformation are shown in Figure S1.

All-Atom MD Simulations

The intimate assembly between neighboring TatA molecules was investigated by means of all-atom MD simulations, without any restraints applied to the postulated salt bridges. The starting structure was obtained from the Gō model, preprocessed with the xleap tool of the AMBER package (Case et al., 2005), and default protonation states were assigned to all residues. All simulations were performed with the sander module of the AMBER package (Case et al., 2005), using the parm03 force field (Duan et al., 2003) to parametrize the protein. A time step of 2 fs was used and the temperature was controlled by using a Langevin thermostat (Uberuaga et al., 2004) with a collision frequency of 5 ps^{-1}.

Mutagenesis of TatA and Analysis by Blue Native Gel Electrophoresis

All mutageneses were carried out by using a QuikChange II Site-Directed Mutagenesis Kit (Agilent, Waldbronn, Germany) according to the protocol of the manufacturer. Oligonucleotide primers (see Table S3) were purchased from Eurofins MWG (Ebersberg, Germany), and the DNA sequence of each mutant was verified by sequencing (GATC Biotech, Konstanz, Germany).

All TatA mutants were overexpressed in *E. coli* BL21 cells (Novagen, Merck, Darmstadt, Germany) in LB medium with 0.2% glucose and kanamycin (50 μg/ml) at 37°C and 220 rpm shaking frequency. Cells were harvested and disrupted by sonication, whereupon Pefabloc SC, phenylmethylsulfonylfluoride, and benzamidine were added as protease inhibitors, and benzonase

for degradation of RNA and DNA. The cell debris and undisrupted cells were removed by centrifugation at 9,000 rpm (19776-H, Sigma Zentrifugen, Osterode, Germany) for 30 min. To harvest the membranes for blue native PAGE, the supernatant was centrifuged at 40,000 rpm (Type 45 Ti, Beckman Coulter, Krefeld, Germany) for 1 hr.

Blue native polyacrylamide gel electrophoresis (BN-PAGE) was performed according to Schägger et al. (Schägger and von Jagow, 1991; Wittig et al., 2006). Please see Extended Experimental Procedures for more details.

SUPPLEMENTAL INFORMATION

Supplemental Information includes Extended Experimental Procedures, four figures, three tables, and one movie and can be found with this article online at http://dx.doi.org/10.1016/j.cell.2012.12.017.

ACKNOWLEDGMENTS

We thank Ralf Heinzmann for the assistance in preparing the Graphical Abstract. A.S.U. and S.L.G. thank the DFG-Center for Functional Nanostructures (TP E1.2 & E3.4). T.H.W. is supported by a YIG grant (KIT Karlsruhe, Germany). M.W. and W.W. acknowledge funding by the HPC Programme of the BW Stiftung. P.R. and A.V.V. thank CINECA for computational support. A.V.V. acknowledges financial support from "Regione Autonoma della Sardegna" through a Research Fellow on fundings "PO Sardegna FSE 2007-2013, L.R.7/2007 Promozione della ricerca scientifica e dell'innovazione tecnologica in Sardegna".

Received: August 18, 2010
Revised: August 20, 2012
Accepted: December 13, 2012
Published: January 17, 2013

REFERENCES

Alder, N.N., and Theg, S.M. (2003). Energetics of protein transport across biological membranes: a study of the thylakoid DeltapH-dependent/cpTat pathway. Cell *112*, 231–242.

Barnett, J.P., Eijlander, R.T., Kuipers, O.P., and Robinson, C. (2008). A minimal Tat system from a gram-positive organism: a bifunctional TatA subunit participates in discrete TatAC and TatA complexes. J. Biol. Chem. *283*, 2534–2542.

Beckstein, O., Denning, E.J., Perilla, J.R., and Woolf, T.B. (2009). Zipping and unzipping of adenylate kinase: atomistic insights into the ensemble of open<—>closed transitions. J. Mol. Biol. *394*, 160–176.

Berks, B.C., Palmer, T., and Sargent, F. (2005). Protein targeting by the bacterial twin-arginine translocation (Tat) pathway. Curr. Opin. Microbiol. *8*, 174–181.

Berks, B.C., Sargent, F., and Palmer, T. (2000). The Tat protein export pathway. Mol. Microbiol. *35*, 260–274.

Berthelmann, F., Mehner, D., Richter, S., Lindenstrauss, U., Lünsdorf, H., Hause, G., and Brüser, T. (2008). Recombinant expression of tatABC and tatAC results in the formation of interacting cytoplasmic TatA tubes in Escherichia coli. J. Biol. Chem. *283*, 25281–25289.

Bonomi, M., Branduardi, D., Bussi, G., Camilloni, C., Provasi, D., Raiteri, P., Donadio, D., Marinelli, F., Pietrucci, F., Broglia, R.A., et al. (2009). PLUMED: A portable plugin for free-energy calculations with molecular dynamics. Comput. Phys. Commun. *180*, 1961–1972.

Brüser, T., and Sanders, C. (2003). An alternative model of the twin arginine translocation system. Microbiol. Res. *158*, 7–17.

Burrack, S., Aberle, D., Bürck, J., Ulrich, A.S., and Meyers, G. (2012). A new type of intracellular retention signal identified in a pestivirus structural glycoprotein. FASEB J. *26*, 3292–3305.

Case, D.A., Cheatham, T.E., 3rd, Darden, T., Gohlke, H., Luo, R., Merz, K.M., Jr., Onufriev, A., Simmerling, C., Wang, B., and Woods, R.J. (2005). The Amber biomolecular simulation programs. J. Comput. Chem. *26*, 1668–1688.

Chan, C.S., Zlomislic, M.R., Tieleman, D.P., and Turner, R.J. (2007). The TatA subunit of Escherichia coli twin-arginine translocase has an N-in topology. Biochemistry *46*, 7396–7404.

Dabney-Smith, C., Mori, H., and Cline, K. (2003). Requirement of a Tha4-conserved transmembrane glutamate in thylakoid Tat translocase assembly revealed by biochemical complementation. J. Biol. Chem. *278*, 43027–43033.

Dabney-Smith, C., Mori, H., and Cline, K. (2006). Oligomers of Tha4 organize at the thylakoid Tat translocase during protein transport. J. Biol. Chem. *281*, 5476–5483.

Dilks, K., Rose, R.W., Hartmann, E., and Pohlschröder, M. (2003). Prokaryotic utilization of the twin-arginine translocation pathway: a genomic survey. J. Bacteriol. *185*, 1478–1483.

Dörr, T., Vulić, M., and Lewis, K. (2010). Ciprofloxacin causes persister formation by inducing the TisB toxin in Escherichia coli. PLoS Biol. *8*, e1000317.

Duan, Y., Wu, C., Chowdhury, S., Lee, M.C., Xiong, G., Zhang, W., Yang, R., Cieplak, P., Luo, R., Lee, T., et al. (2003). A point-charge force field for molecular mechanics simulations of proteins based on condensed-phase quantum mechanical calculations. J. Comput. Chem. *24*, 1999–2012.

Frank, R.A., Pratap, J.V., Pei, X.Y., Perham, R.N., and Luisi, B.F. (2005). The molecular origins of specificity in the assembly of a multienzyme complex. Structure *13*, 1119–1130.

Fröbel, J., Rose, P., and Müller, M. (2012). Twin-arginine-dependent translocation of folded proteins. Philos. Trans. R. Soc. Lond. B Biol. Sci. *367*, 1029–1046.

Gō, N., and Scheraga, H.A. (1976). On the Use of Classical Statistical Mechanics in the Treatment of Polymer Chain Conformation. Macromolecules *9*, 535–542.

Gohlke, U., Pullan, L., McDevitt, C.A., Porcelli, I., de Leeuw, E., Palmer, T., Saibil, H.R., and Berks, B.C. (2005). The TatA component of the twin-arginine protein transport system forms channel complexes of variable diameter. Proc. Natl. Acad. Sci. USA *102*, 10482–10486.

Gouffi, K., Gérard, F., Santini, C.-L., and Wu, L.-F. (2004). Dual topology of the Escherichia coli TatA protein. J. Biol. Chem. *279*, 11608–11615.

Hess, B., Kutzner, C., van der Spoel, D., and Lindahl, E. (2008). GROMACS 4: Algorithms for Highly Efficient, Load-Balanced, and Scalable Molecular Simulation. J. Chem. Theory Comput. *4*, 435–447.

Hu, Y., Zhao, E., Li, H., Xia, B., and Jin, C. (2010). Solution NMR structure of the TatA component of the twin-arginine protein transport system from gram-positive bacterium Bacillus subtilis. J. Am. Chem. Soc. *132*, 15942–15944.

Jack, R.L., Sargent, F., Berks, B.C., Sawers, G., and Palmer, T. (2001). Constitutive expression of Escherichia coli tat genes indicates an important role for the twin-arginine translocase during aerobic and anaerobic growth. J. Bacteriol. *183*, 1801–1804.

Jongbloed, J.D.H., Grieger, U., Antelmann, H., Hecker, M., Nijland, R., Bron, S., and van Dijl, J.M. (2004). Two minimal Tat translocases in Bacillus. Mol. Microbiol. *54*, 1319–1325.

Kim, H., Hsin, J., Liu, Y., Selvin, P.R., and Schulten, K. (2010). Formation of salt bridges mediates internal dimerization of myosin VI medial tail domain. Structure *18*, 1443–1449.

Lange, C., Müller, S.D., Walther, T.H., Bürck, J., and Ulrich, A.S. (2007). Structure analysis of the protein translocating channel TatA in membranes using a multi-construct approach. Biochim. Biophys. Acta *1768*, 2627–2634.

Larkin, M.A., Blackshields, G., Brown, N.P., Chenna, R., McGettigan, P.A., McWilliam, H., Valentin, F., Wallace, I.M., Wilm, A., Lopez, R., et al. (2007). Clustal W and Clustal X version 2.0. Bioinformatics *23*, 2947–2948.

Leake, M.C., Greene, N.P., Godun, R.M., Granjon, T., Buchanan, G., Chen, S., Berry, R.M., Palmer, T., and Berks, B.C. (2008). Variable stoichiometry of the TatA component of the twin-arginine protein transport system observed by in vivo single-molecule imaging. Proc. Natl. Acad. Sci. USA *105*, 15376–15381.

Lee, P.A., Buchanan, G., Stanley, N.R., Berks, B.C., and Palmer, T. (2002). Truncation analysis of TatA and TatB defines the minimal functional units required for protein translocation. J. Bacteriol. *184*, 5871–5879.

Li, Y.D., Zhou, Z., Lv, L.X., Hou, X.P., and Li, Y.Q. (2009). New approach to achieve high-level secretory expression of heterologous proteins by using Tat signal peptide. Protein Pept. Lett. *16*, 706–710.

Mack, J.W., Steven, A.C., and Steinert, P.M. (1993). The mechanism of interaction of filaggrin with intermediate filaments. The ionic zipper hypothesis. J. Mol. Biol. *232*, 50–66.

Mande, S.S., Sarfaty, S., Allen, M.D., Perham, R.N., and Hol, W.G. (1996). Protein-protein interactions in the pyruvate dehydrogenase multienzyme complex: dihydrolipoamide dehydrogenase complexed with the binding domain of dihydrolipoamide acetyltransferase. Structure *4*, 277–286.

Mori, H., and Cline, K. (2001). Post-translational protein translocation into thylakoids by the Sec and Delta pH-dependent pathways. Biochim. Biophys. Acta *1541*, 80–90.

Müller, S.D., De Angelis, A.A., Walther, T.H., Grage, S.L., Lange, C., Opella, S.J., and Ulrich, A.S. (2007). Structural characterization of the pore forming protein TatAd of the twin-arginine translocase in membranes by solid-state ^{15}N-NMR. Biochim. Biophys. Acta *1768*, 3071–3079.

Musafia, B., Buchner, V., and Arad, D. (1995). Complex salt bridges in proteins: statistical analysis of structure and function. J. Mol. Biol. *254*, 761–770.

Musser, S.M., and Theg, S.M. (2000). Characterization of the early steps of OE17 precursor transport by the thylakoid DeltapH/Tat machinery. Eur. J. Biochem. *267*, 2588–2598.

Noel, J.K., Whitford, P.C., Sanbonmatsu, K.Y., and Onuchic, J.N. (2010). SMOG@ctbp: simplified deployment of structure-based models in GROMACS. Nucleic Acids Res. *38*(Web Server issue), W657–61.

Oates, J., Barrett, C.M., Barnett, J.P., Byrne, K.G., Bolhuis, A., and Robinson, C. (2005). The Escherichia coli twin-arginine translocation apparatus incorporates a distinct form of TatABC complex, spectrum of modular TatA complexes and minor TatAB complex. J. Mol. Biol. *346*, 295–305.

Palmer, T., and Berks, B.C. (2003). Moving folded proteins across the bacterial cell membrane. Microbiology *149*, 547–556.

Palmer, T., Sargent, F., and Berks, B.C. (2005). Export of complex cofactor-containing proteins by the bacterial Tat pathway. Trends Microbiol. *13*, 175–180.

Paulmann, M., Arnold, T., Linke, D., Özdirekcan, S., Kopp, A., Gutsmann, T., Kalbacher, H., Wanke, I., Schuenemann, V.J., Habeck, M., et al. (2012). Structure-activity analysis of the dermcidin-derived peptide DCD-1L, an anionic antimicrobial peptide present in human sweat. J. Biol. Chem. *287*, 8434–8443.

Pop, O., Martin, U., Abel, C., and Müller, J.P. (2002). The twin-arginine signal peptide of PhoD and the TatAd/Cd proteins of Bacillus subtilis form an autonomous Tat translocation system. J. Biol. Chem. *277*, 3268–3273.

Porcelli, I., de Leeuw, E., Wallis, R., van den Brink-van der Laan, E., de Kruijff, B., Wallace, B.A., Palmer, T., and Berks, B.C. (2002). Characterization and membrane assembly of the TatA component of the Escherichia coli twin-arginine protein transport system. Biochemistry *41*, 13690–13697.

Robinson, C., and Bolhuis, A. (2004). Tat-dependent protein targeting in prokaryotes and chloroplasts. Biochim. Biophys. Acta *1694*, 135–147.

Rosenberg, K.J., Ross, J.L., Feinstein, H.E., Feinstein, S.C., and Israelachvili, J. (2008). Complementary dimerization of microtubule-associated tau protein: Implications for microtubule bundling and tau-mediated pathogenesis. Proc. Natl. Acad. Sci. USA *105*, 7445–7450.

Sargent, F., Gohlke, U., De Leeuw, E., Stanley, N.R., Palmer, T., Saibil, H.R., and Berks, B.C. (2001). Purified components of the Escherichia coli Tat protein transport system form a double-layered ring structure. Eur. J. Biochem. *268*, 3361–3367.

Schägger, H., and von Jagow, G. (1991). Blue native electrophoresis for isolation of membrane protein complexes in enzymatically active form. Anal. Biochem. *199*, 223–231.

Schittek, B., Hipfel, R., Sauer, B., Bauer, J., Kalbacher, H., Stevanovic, S., Schirle, M., Schroeder, K., Blin, N., Meier, F., et al. (2001). Dermcidin: a novel human antibiotic peptide secreted by sweat glands. Nat. Immunol. *2*, 1133–1137.

Steinbrecher, T., Prock, S., Reichert, J., Wadhwani, P., Zimpfer, B., Bürck, J., Berditsch, M., Elstner, M., and Ulrich, A.S. (2012). Peptide-lipid interactions of the stress-response peptide TisB that induces bacterial persistence. Biophys. J. *103*, 1460–1469.

Tews, B.A., and Meyers, G. (2007). The pestivirus glycoprotein E^{rns} is anchored in plane in the membrane via an amphipathic helix. J. Biol. Chem. *282*, 32730–32741.

Unoson, C., and Wagner, E.G.H. (2008). A small SOS-induced toxin is targeted against the inner membrane in Escherichia coli. Mol. Microbiol. *70*, 258–270.

Uberuaga, B.P., Anghel, M., and Voter, A.F. (2004). Synchronization of trajectories in canonical molecular-dynamics simulations: observation, explanation, and exploitation. J. Chem. Phys. *120*, 6363–6374.

van der Ploeg, R., Barnett, J.P., Vasisht, N., Goosens, V.J., Pöther, D.C., Robinson, C., and van Dijl, J.M. (2011). Salt sensitivity of minimal twin arginine translocases. J. Biol. Chem. *286*, 43759–43770.

Walther, T.H., Grage, S.L., Roth, N., and Ulrich, A.S. (2010). Membrane alignment of the pore-forming component $TatA_{(d)}$ of the twin-arginine translocase from Bacillus subtilis resolved by solid-state NMR spectroscopy. J. Am. Chem. Soc. *132*, 15945–15956.

Warren, G., Oates, J., Robinson, C., and Dixon, A.M. (2009). Contributions of the transmembrane domain and a key acidic motif to assembly and function of the TatA complex. J. Mol. Biol. *388*, 122–132.

Waterhouse, A.M., Procter, J.B., Martin, D.M.A., Clamp, M., and Barton, G.J. (2009). Jalview Version 2—a multiple sequence alignment editor and analysis workbench. Bioinformatics *25*, 1189–1191.

Westermann, M., Pop, O.I., Gerlach, R., Appel, T.R., Schlörmann, W., Schreiber, S., and Müller, J.P. (2006). The TatAd component of the Bacillus subtilis twin-arginine protein transport system forms homo-multimeric complexes in its cytosolic and membrane embedded localisation. Biochim. Biophys. Acta *1758*, 443–451.

White, G.F., Schermann, S.M., Bradley, J., Roberts, A., Greene, N.P., Berks, B.C., and Thomson, A.J. (2010). Subunit organization in the TatA complex of the twin arginine protein translocase: a site-directed EPR spin labeling study. J. Biol. Chem. *285*, 2294–2301.

Whitford, P.C., Noel, J.K., Gosavi, S., Schug, A., Sanbonmatsu, K.Y., and Onuchic, J.N. (2009). An all-atom structure-based potential for proteins: bridging minimal models with all-atom empirical forcefields. Proteins *75*, 430–441.

Wittig, I., Braun, H.P., and Schägger, H. (2006). Blue native PAGE. Nat. Protoc. *1*, 418–428.

Zhang, L., Zhu, Z., Jing, H., Zhang, J., Xiong, Y., Yan, M., Gao, S., Wu, L.F., Xu, J., and Kan, B. (2009). Pleiotropic effects of the twin-arginine translocation system on biofilm formation, colonization, and virulence in Vibrio cholerae. BMC Microbiol. *9*, 114.